Princeton Plasma Physics Laboratory

PPPL- 4827

PPPL- 4827

Perturbative Study of Energetic Particle Redistribution by Alfven Eigenmodes in ITER

N.N. Gorelenkov and R.B. White

October, 2012

PPPL PRINCETON PLASMA PHYSICS LABORATORY

Prepared for the U.S. Department of Energy under Contract DE-AC02-09CH11466.

Princeton Plasma Physics Laboratory
Report Disclaimers

Full Legal Disclaimer

Trademark Disclaimer

PPPL Report Availability

Princeton Plasma Physics Laboratory:

http://www.pppl.gov/techreports.cfm

Office of Scientific and Technical Information (OSTI):

http://www.osti.gov/bridge

Related Links:

U.S. Department of Energy

Office of Scientific and Technical Information

Fusion Links

Perturbative study of energetic particle redistribution by Alfvén eigenmodes in ITER

N. N. Gorelenkov, R. B. White[1]

[1]*Plasma Physics Laboratory, Princeton University,*

P.O.Box 451, Princeton, New Jersey 08543

Abstract

The modification of particle distributions by magnetohydrodynamic modes is an important topic for magnetically confined plasmas. Low amplitude modes are known to be capable of producing significant modification of injected neutral beam profiles. Flattening of a distribution due to phase mixing in an island or due to portions of phase space becoming stochastic is a process extremely rapid on the time scale of equilibrium parameter changes in an experiment. In this paper we examine the effect of toroidal Alfvén eigenmodes (TAE) and reversed shear Alfvén eigenmodes (RSAE) in ITER on alpha particle and injected beam distributions using theoretically predicted mode amplitudes using perturbative linear theory. It is found that for the equilibrium of a hybrid scenario even at ten times the predicted saturation level the modes have negligible effect on these distributions. A strongly reversed shear (or advanced) scenario, having a spectrum of modes that are much more global, is somewhat more susceptible to induced loss due to mode resonance, with alpha particle losses of over one percent with predicted amplitudes and somewhat larger with the assistance of toroidal field ripple. The elevated q profile contributes to stronger TAE (RSAE) drive and more unstable modes. An analysis of the existing mode-particle resonances is carried out to determine which modes are responsible for the profile modification and induced loss. We find that losses are entirely due to resonance with the counter-moving and trapped particle populations, with co-moving passing particles participating in resonances only deep within the plasma core and not leading to loss.

PACS numbers: 52.25.Fi, 52.25.Gj

I. INTRODUCTION

The resonant interaction of magnetohydrodynamic (MHD) modes with a particle distribution can produce significant modification of the distribution and even induce large scale particle loss through profile avalanche, and is an important topic for magnetically confined plasmas. Low amplitude Alfvén modes are known to be capable of producing significant modification of injected neutral beam profiles[1–5]. Since magnetic field ripple is a strong function of position, increasing rapidly near the plasma edge, a broadened profile can lead to an increase of stochastic trapped particle ripple loss[6]. In this work we examine ITER[7] equilibria for unstable toroidal Alfvén eigenmodes (TAE) and reversed shear Alfvén eigenmodes (RSAE) capable of growing to an amplitude producing significant modification of the alpha particle or injected beam profiles. We have examined several ITER equilibria, looking for those unstable to TAE and RSAE modes, produced either by the alpha particle or the beam distribution. It is found that generally most modes are stable, so the number of unstable modes is small. The saturation amplitudes of the unstable modes are determined theoretically. The cases most susceptible to TAE instability have a region of reversed shear. A previous work[8] using *ad hoc* estimations for mode amplitude revealed no losses due to TAE or RSAE modes. The present analysis, using theoretically predicted mode amplitudes, is in agreement with these results for hybrid scenario equilibria, where the most unstable modes have a toroidal mode number of $n = 8$. In contrast to this a case with severe reversed shear, and a much larger spectrum of radially wider modes with n ranging from 1 to 14 does exhibit some induced loss. In section II we outline the theory used to obtain saturated mode amplitudes. In section III we review the methods used to determine the mode-particle resonances responsible for producing profile modification. In section IV we describe the toroidal field ripple and the particle distributions. In section V we discuss the hybrid scenario equilibrium, and in section VI we examine an equilibrium with strongly reversed shear. Conclusions are given in section VII.

II. MODE SATURATION

In previous work it has been possible to verify theoretically predicted mode spectra and amplitudes with experimental observations for the study of the effect of these modes on

particle distributions [2, 3]. The same study for ITER limits us to a theoretical prediction of spectra and saturation amplitudes. The saturation of TAE modes, driven unstable by a high energy particle distribution is due to a balance of nonlinear growth and damping effects mediated by the appropriate modifications of the fast ion distribution near the resonances.

We employ the nonlinear theory of kinetic instabilities near threshold to calculate the saturation level of TAE amplitudes assuming that each resonance of the unstable mode with energetic ions is not overlapped with another mode in phase space[9] The theory is embedded for routine runs into the hybrid MHD/kinetic NOVA-K code[10]. This code is coupled to nonlinear simulation runs and resonance analysis using the guiding center code ORBIT[2, 3]. This procedure is used here for the first time to produce the amplitude level for TAE spectra in the equilibria describing ITER plasmas and to predict the effect of such modes.

The amplitudes are computed in NOVA-K balancing the background damping with the linear and nonlinear fast ion drives and averaging them over phase space. The expression for the TAE amplitudes is derived in two asymptotic regimes connected to each other using an interpolation formula, the asymptotic local limits having been obtained independently. The two regimes differ in the ratio ω_b/ν_{eff}, which is much smaller or larger than unity, where ν_{eff} is the effective collision frequency and ω_b is the particle trapping frequency in the perturbed fields of the mode[10]. The interpolation formula is

$$\frac{\gamma_d}{\gamma_L} = \overline{\left[1 + 0.57U\left(\Gamma\right) / \left(1 + 1.45/U\left(\Gamma\right)\right)^{1/3}\right]^{-1}}, \tag{1}$$

where the bar means phase space averaging over the mode structure with the local contribution to the growth rate used as weighting factor in the averaging, Γ is the phase space coordinate of the particle location, and $U\left(\Gamma\right) = \left(\omega_b/\nu_{eff}\right)^3$.

It was noted that the above equation works well especially in the near threshold regime whereas in the regime when the amplitude of the mode is strong it slightly deviates from the numerically obtained amplitudes. In the regimes of interest the most relevant case is when $\gamma_d/\gamma_L \lesssim 1$ where the application of Eq. 1 is justified.

III. RESONANCES

Instability is not sufficient to predict the effect of a given mode on the driving particle distribution. It is necessary to know the mode amplitude, the size of the phase space islands produced by the saturated mode, and to ascertain whether the possibility of overlap can lead to avalanche and large scale profile changes. A numerical simulation by following particle trajectories in the presence of a spectrum of modes reveals losses and profile modification, but does not establish which modes are responsible for the interactions.

The interaction of particle distributions and MHD modes can be studied in the guiding center approximation. Using the guiding center drift approximation a particle orbit in an axisymmetric system is completely described by the values of the toroidal canonical momentum P_ζ, the energy E and the magnetic moment μ. Particle spatial coordinates of the guiding center are given by ψ_p, θ, ζ, respectively the poloidal flux coordinate, and the poloidal and toroidal angles. The magnetic field is given by

$$\vec{B} = g\nabla\zeta + I\nabla\theta + \delta\nabla\psi_p, \tag{2}$$

and in an axisymmetric equilibrium using Boozer coordinates g and I are functions of ψ_p only[15].

The guiding center Hamiltonian is

$$H = \rho_\parallel^2 B^2/2 + \mu B + \Phi, \tag{3}$$

where $\rho_\parallel = v_\parallel/B$ is the normalized parallel velocity, $v_\parallel$ is the particle velocity parallel to the magnetic field, μ is the magnetic moment, and Φ the electric potential. Canonical momenta are

$$P_\zeta = g\rho_\parallel - \psi_p, \qquad P_\theta = \psi + \rho_\parallel I, \tag{4}$$

where ψ is the toroidal flux, with $d\psi/d\psi_p = q(\psi_p)$, the field line helicity. The equations of motion in Hamiltonian form are

$$\begin{aligned} \dot{\theta} &= \frac{\partial H}{\partial P_\theta} \qquad & \dot{P}_\theta &= -\frac{\partial H}{\partial \theta} \\ \dot{\zeta} &= \frac{\partial H}{\partial P_\zeta} \qquad & \dot{P}_\zeta &= -\frac{\partial H}{\partial \zeta}. \end{aligned} \tag{5}$$

Equations for advancing particle positions in time, also in the presence of flute-like perturbations of the form $\delta\vec{B} = \nabla \times \alpha\vec{B}$ with $\vec{B}$ the equilibrium field and α a function of ψ_p, θ, ζ,

and t can easily be derived[15]. The guiding center equations including MHD perturbations are realized using a fourth order Runge-Kutta algorithm in the code ORBIT[16].

The magnetic perturbation $\delta\vec{B} = \nabla \times \alpha\vec{B}$ exactly represents the cross field magnitude of the perturbation, responsible for producing magnetic islands if the mode is non ideal, and most important for the production of resonances for the ideal modes considered in this work. It is simply related to the ideal MHD displacement $\vec{\xi}$. In addition, using α to describe the perturbation introduces an electric field parallel to $\vec{B}$ proportional to the mode frequency. Since this is forbidden in ideal MHD, a potential must be introduced to cancel this field if the α form is to represent an ideal perturbation. Expand α in a Fourier series of the form $\alpha = \sum_{m,n} \alpha_{m,n}(\psi_p) sin(n\zeta - m\theta - \omega t)$. Now add an electric potential Φ to cancel the parallel electric field induced by $d\vec{B}/dt$, with

$$\sum_{m,n} \omega B \alpha_{m,n} sin(n\zeta - m\theta - \omega t) - \vec{B} \cdot \nabla\Phi/B = 0, \tag{6}$$

giving a very simple expression if one uses Boozer coordinates with I independent of θ, $(gq + I)\omega\alpha_{mn} = (nq - m)\Phi_{mn}$. We also find that alpha is simply related to the cross field component of the ideal displacement.

$$\alpha_{mn} = \frac{(m/q - n)}{(mg + nI)} \xi^{\psi}_{mn}. \tag{7}$$

In the present version of NOVA-K the data for the $\xi(\psi_p)$ eigenfunctions is passed to ORBIT rather than the data for $\alpha_{mn}(\psi_p)$. This is numerically preferable because of the singularity arising when constructing $\xi(\psi_p)$ from $\alpha_{mn}(\psi_p)$ due to numerical misalignment of the zeros in $nq - m$ and $\alpha_{mn}(\psi_p)$.

The magnetic moment μ is conserved by the interaction of a particle with a mode with frequency much smaller than the cyclotron frequency, so only P_ζ and E are modified by interaction with it. For a perturbation of a single n the Hamiltonian is a function of the combination $n\zeta - \omega t$. Then from $\dot{P}_\zeta = -\frac{\partial H}{\partial \zeta}$ and $\frac{dE}{dt} = \frac{\partial H}{\partial t}$, we find that for fixed n we have $E - P_\zeta \omega/n = constant$ in time, simply a statement of energy conservation in the mode frame.

It is fairly easy to assess the effect of a given mode on a particle distribution by examining a Poincaré plot for a particular choice of either co-passing and trapped or counter-passing particles, which we refer to as a kinetic Poincaré plot to distinguish it from a plot of the magnetic field. Points are plotted in the poloidal cross section whenever $n\zeta - \omega_n t = 2\pi k$

with k integer. The toroidal motion then gives successive Poincaré points in the poloidal cross section ψ_p, θ, or better, since P_ζ is constant in the absence of perturbations, the P_ζ, θ plane. Individual modes produce islands in the phase space of the particle orbits, which through phase mixing produce local flattening of the particle distribution. In previous work methods have been developed for scanning the whole distribution space to discover important resonances[17, 18], and these techniques have been used to find the locations of resonance islands produced by a given mode spectrum for ITER discharges.

Only through resonance can small amplitude waves modify a particle distribution. Without resonance the trajectories in phase space occupy Kolmogorov Arnold Moser[14] (KAM) surfaces that are topologically equivalent to nonintersecting planes. Excursion from the original drift surfaces is proportional to the mode amplitude for nonresonant motion, but proportional to the square root of the amplitude for resonances, and thus for small amplitudes modes only resonances are important. A Poincaré point, indicating one passage through the wave, which is a function of $n\zeta - m\theta - \omega_n t$, occurs when $n\zeta - \omega_n t = 2\pi k$, with k integer. For there to be m' periodic fixed points in θ we also require $\Delta\theta = 2\pi l/m'$ between successive points with l integer. Here m' is the number of islands in a poloidal cross section Poincaré plot. Thus the particle can return to receive the same impulse from the wave by passing through the fixed finite set of θ values, for those values of m in the perturbation that are also consistent with the number of islands poloidally. The helicity of the resonance is then

$$h(P_\zeta, E, \mu) = \frac{\Delta\zeta - \omega_n \Delta t/n}{\Delta\theta} = \frac{m'}{nl}, \tag{8}$$

which must be rational, where $\Delta\zeta$, $\Delta\theta$, Δt refer to one transit. For qualitative understanding only, use a low energy approximation for passing particles with $\Delta\zeta = q\Delta\theta$. Further using a large aspect ratio approximation find $R\Delta\zeta = v_\parallel \Delta t$ giving

$$h = q\left[1 - \frac{\omega_n R}{n v_\parallel}\right]. \tag{9}$$

This equation displays the strong effect of the parallel velocity on the existence of resonances.

IV. TOROIDAL FIELD RIPPLE AND PARTICE DISTRIBUTIONS

We have also included the effect of toroidal magnetic field ripple, since it can assist in producing losses of trapped high energy particles. ITER ripple is given by a document of

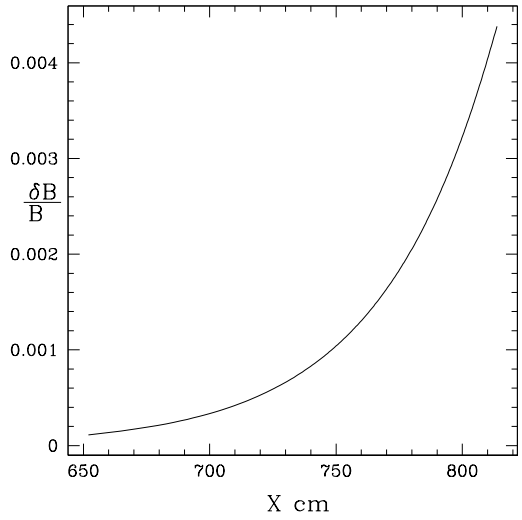

FIG. 1: ITER ripple magnitude along the outer midplane.

the database of the magnetic field produced by TF coils, Ferromagnetic Inserts, and Test Blanket Modules magnetized in toroidal and poloidal magnetic fields (15MA DT scenario at burn)[7]. The data was fit by the following expression

$$\frac{\delta B}{B} = d_0 e^{\sqrt{(x-x_r)^2+b_r z^2}/w} sin(N\phi), \tag{10}$$

with X the major radius position, and Z the vertical coordinate. For ITER N = 18, $x_r = 500$ cm, $w = 43.5$ cm, $d_0 = 3.16 \times 10^{-6}$, $b_r = 0.49$. The magnitude of the ripple along the outer midplane is shown in Fig. 1. Only near the plasma edge can the ripple be effective in promoting trapped particle loss.

Monte Carlo representations of the expected slowing down alpha particle and beam particle distributions were obtained from TRANSP[11, 12] for the discharges used. The energy distributions are shown in Fig. 2. The distributions are fitted analytically for use in NOVA-K and directly provided for ORBIT simulations as lists of one million or more particles.

V. HYBRID SCENARIO

It is generally found that only equilibria with flat, or even reversed q profiles have a significant spectrum of unstable TAE modes. The equilibrium and q profile for one hybrid scenario case 40500T02 at t=350 sec, extensively studied in [13], are shown in Fig. 3.

Shown in Fig. 4 are the poloidal harmonics of an unstable TAE mode in the discharge

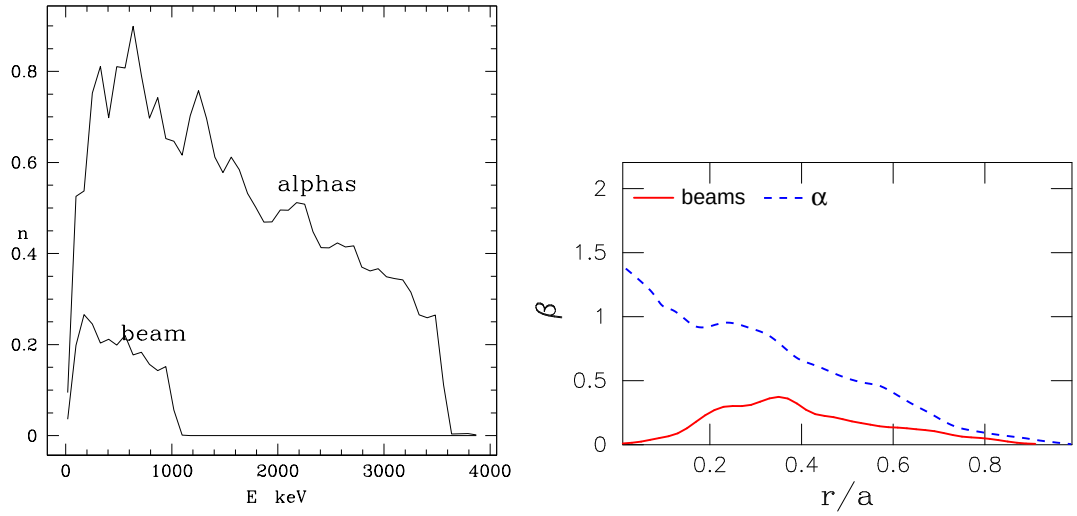

FIG. 2: Alpha particle and beam distributions. At left the energy distributions from the Monte Carlo particle lists, with n the density, scale arbitrary but equal for the two species, at right the radial profiles.

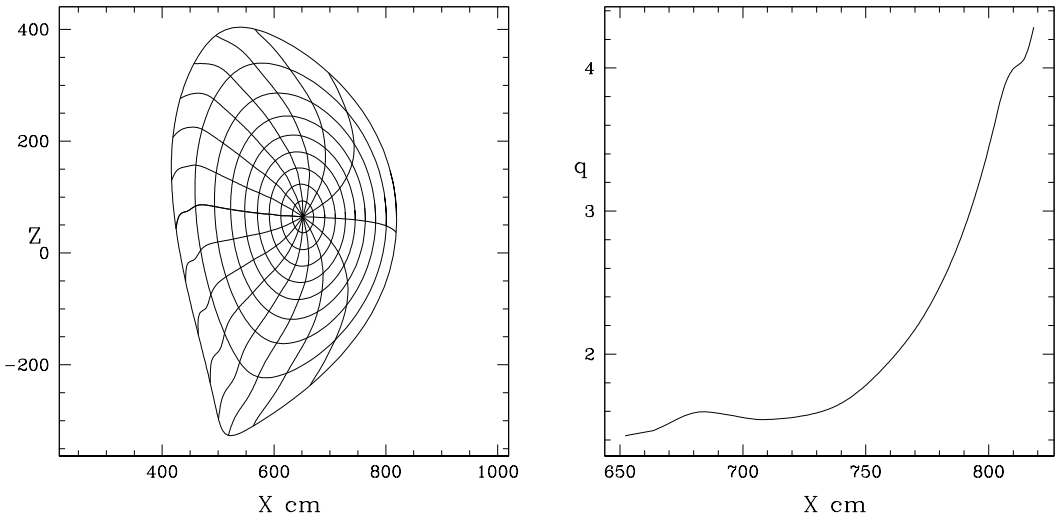

FIG. 3: ITER equilibrium and q profile for a hybrid scenario discharge.

shown in Fig. 3, with a frequency of 56.5 kHz, toroidal mode number $n = 8$, and poloidal harmonics ranging from $m = 10$ to 18. The magnitudes of the ideal displacement ξ are in centimeters with a maximum value of $1.5 \times 10^{-3} cm$. Note that the mode is restricted to the range of flux values corresponding to the region of reversed shear. No unstable global modes were observed due to strong edge continuum and trapped electron collisional dampings.

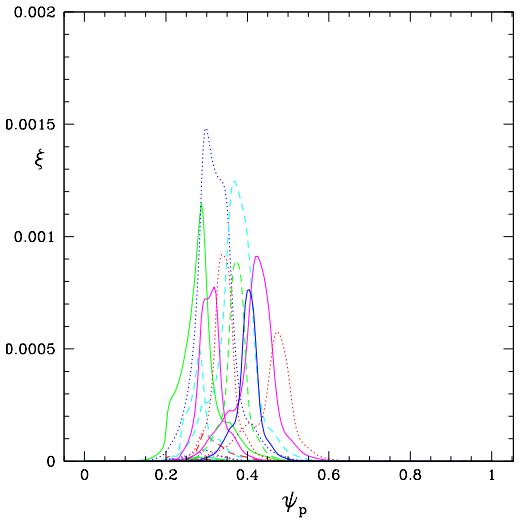

FIG. 4: Saturated TAE mode harmonics, for modes appearing in the hybrid scenario, $n = 8$, $10 \leq m \leq 18$, f = 56.5 kHz. The magnitude of ξ is in centimeters.

Shown in Fig. 5, is a section of the E, P_ζ plane from 1000 to 3000 keV showing all resonances for alpha particles with $\mu B_0 = 100keV$, *ie* deeply passing particles. Similar results are found for all values of μB_0 and hence pitch. The nearly vertical lines are domain boundaries for particle types, the far left line being the last closed flux surface (W) and the far right line the magnetic axis (A). See [17, 18] or [15] for a more complete description of these boundaries and the methods used in finding resonance locations.

Such resonances typically exist over a large range of energy, as is clearly shown, but induced particle motion by the mode is only along lines given by $E - P_\zeta \omega/n = constant$, and only within a resonance, not along the nearly vertical resonance surfaces. One of these lines along which the mode operates is shown between 2500 and 2800 keV, labelled P in the E, P_ζ plane. Also shown is a Poincaré plot of the alpha particle phase space in the presence of the TAE mode along this line.

The resonance with the largest phase space island is the 12 island chain on the far right, which exists for the full energy range examined, almost from 1 MeV to 3 MeV. Over this whole range the island widths are small and approximately constant, as shown in the Poincaré plot of Fig. 5. Note that the range of P_ζ along which the Poincaré plots are shown is not the whole plasma cross section, but includes those values for which the mode amplitude is significant. For these plots the mode is that of Fig. 4, with the theoretically

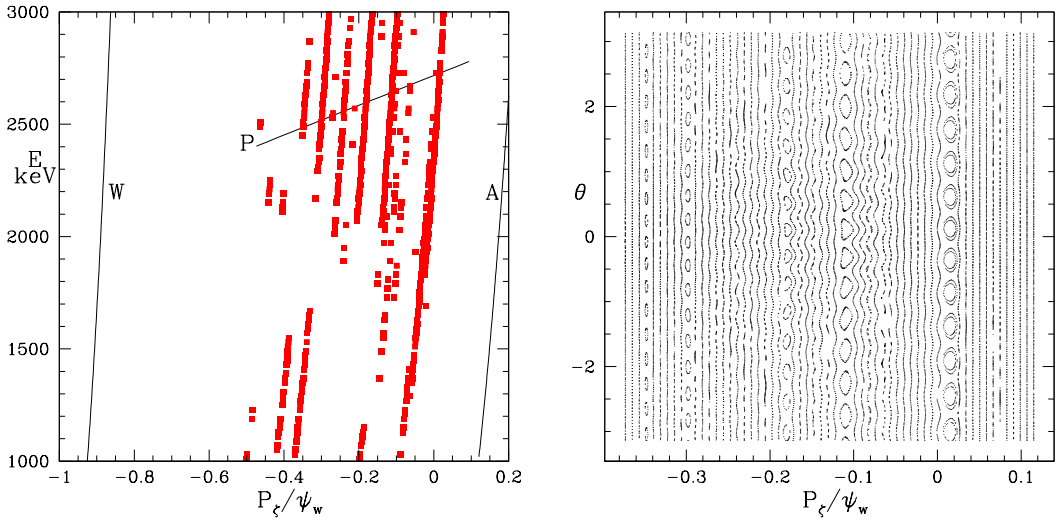

FIG. 5: Resonant modification of the alpha particle distribution with mode amplitude 10 times predicted saturation level for the mode of Fig. 4. The figure on the left shows the E, P_ζ plane from 1000 to 3000 keV, $\mu B_0 = 100keV$, with all resonances marked. The plasma edge is marked W (wall), the axis A. On the right is a kinetic Poincaré plot along the line $E - P_\zeta\omega/n = constant$ shown in the E, P_ζ plane and labelled P. The distribution consists entirely of co-passing particles.

predicted saturated amplitude multiplied by a factor of 10. Even multiplied by a factor of 10 the perturbations produce only very small islolated islands, on the order of one millimeter in width, with minimal possibility of modification of the distribution. Island size scales as the square root of the mode amplitude, so these resonances are about one third this size if the calculated perturbation amplitudes are used, and can be seen only using local restricted Poincaré plots. In addition, the cyclotron radius of the alpha particles in this equilibrium is approximately 3 cm, so the effect of these phase space islands would be additionally diminished by the cyclotron motion as the mode inversed radial wavevector is comparable with the gyroradius, which is not in ORBIT simulations.

Similar results are obtained for the beam particle distribution, again with islands too small to produce a significant modification of the distribution.

VI. ADVANCED, OR REVERSED SHEAR SCENARIO

We now consider an advanced scenario equilibrium with strong shear reversal, where one can expect the largest spectrum of TAE modes to occur The equilibrium and q profile for

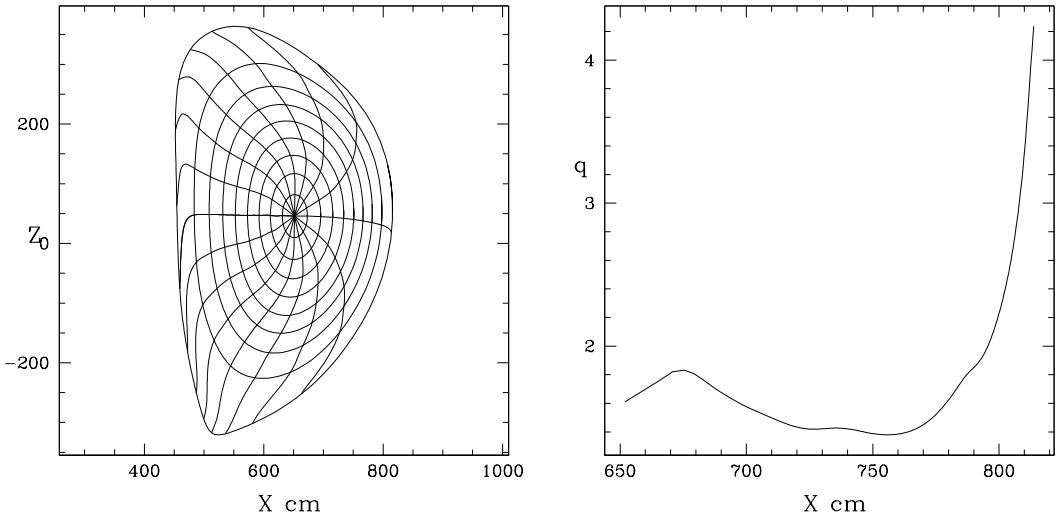

FIG. 6: Reversed shear equilibrium and q profile along the outer midplane.

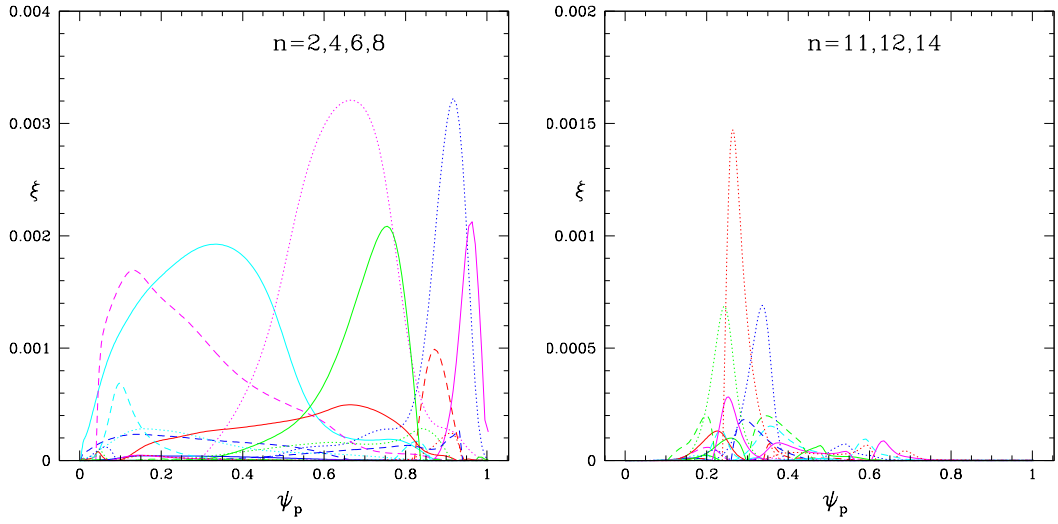

FIG. 7: Examples of saturated TAE mode harmonics in the reversed shear equilibrium. Modes present had toroidal and poloidal mode numbers in the range $n = 1 - 14$, $1 \leq m \leq 146$. for a full list of the unstable modes see Table 1. The magnitude of ξ is in centimeters.

scenario case 40000B11 at 250 *sec*, a strongly reversed shear equilibrium is shown in Fig. 6. In Fig. 7 are shown some of the TAE modes resulting in this equilibrium. Some of the modes with low toroidal mode numbers (n) are rather global in extent, and modes with higher n values are more localized. Unstable modes with significant magnitude have n values ranging from 1 to 14, with typically eight poloidal harmonics for each mode. The complete harmonic

structure of these instabilities is listed in Table I. A total of 131 poloidal harmonics were present in the numerical simulations with ORBIT.

We note that the advanced scenario is relatively more unstable to AEs due to in part the elevated q profile and wide region of near zero shear. This is an important factor to include in the analysis of such plasmas especially when this low shear region is located near the strongest gradient of the α particle pressure profile.

In Fig. 8 is shown the total loss versus TAE amplitude in the reversed shear equilibrium, where $A = 1$ is the value computed in NOVA-K, giving losses of a little over one percent in a simulation of 4 $msec$. All harmonics are multiplied by the same factor A for these simulations. The losses increase much more rapidly than linearly with mode amplitude because of stochastization caused by mode overlap. There are a sufficient number of localized resonances so that an increase in amplitude can lead to island overlap and stochastic redistribution of beam and alpha particles. More consistent analysis of saturation amplitudes in the presence of mode overlap may come from a quasi-linear theory, which is beyond the scope of this paper. But for the present work this is not relevant, since islands are small enough that overlap of islands due to a single mode does not occur. The overlap of islands due to two modes of different frequencies, examined in [17], is a significantly more complicated problem.

Table I. Modes in the Reversed Shear Scenario

Mode	harmonics	Amplitude	kHz
1	1/1 - 7/1	1.7×10^{-2}	137
2	9/2 - 17/2	3.2×10^{-3}	156
3	17/2 - 23/2	1.7×10^{-3}	72.9
4	26/4 - 34/4	6.9×10^{-4}	148
5	37/6 - 45/6	2.3×10^{-3}	85.3
6	49/8 - 57/8	9.8×10^{-4}	154
7	62/11 - 70/11	6.9×10^{-4}	148
8	71/12 - 79/12	6.9×10^{-4}	156
9	80/12 - 88/12	1.5×10^{-3}	150
10	90/12 - 98/12	2.0×10^{-3}	79.3
11	99/12 - 107/12	2.1×10^{-4}	71.4
12	110/14 - 118/14	8.8×10^{-4}	148
13	120/14 - 128/14	9.8×10^{-4}	151
14	128/14 - 136/14	3.4×10^{-4}	144
15	138/14 - 146/14	1.5×10^{-3}	84.2

There is some effect of ITER field ripple on the mode induced loss. Also shown in Fig. 8 is the original particle beta distribution in minor radius as well as the loss distribution of particles in the reversed shear equilibrium as a function of perpendicular energy μB and total energy, with and without ripple. The inclusion of ripple produces larger losses in the region of large μB, corresponding to trapped particles, which are susceptible to stochastic ripple transport. The ripple has an effect primarily on the loss channel of particles with energy a little over 2 MeV and with μB greater than 2 MeV.

From Fig. 8 we see that losses are peaked at $\mu B \simeq 800keV$ and at $\mu B \simeq 1700keV$. We now turn to an examination of the resonances produced by these modes in order to understand the loss process, examining only these two values of μB where the losses are concentrated. ORBIT produces plots of the location of resonances in the plane of P_ζ, E for fixed μ for individual modes, consisting of a single n value and frequency, but including all poloidal harmonics[17, 18]. Losses turn out to be produced by very few of the modes involved, most modes only giving rise to profile modification deep within the plasma.

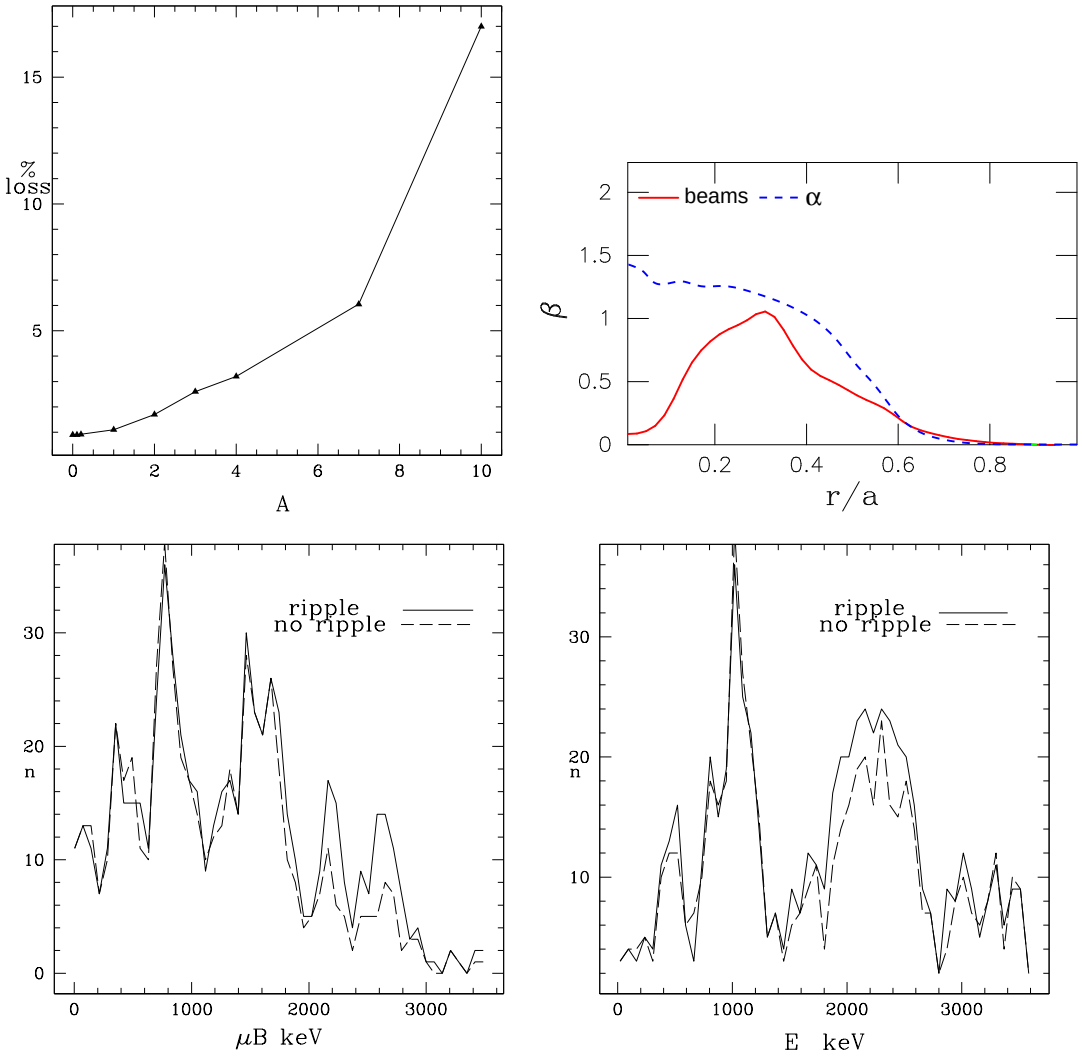

FIG. 8: Top left, loss vs TAE amplitude, with $A = 1$ the value computed by NOVA-K, giving a loss of slightly over one percent in a period of 4 $msec$. Top right is the radial distributions of beam and alpha particle beta. The lower plots show histograms of loss vs μB and E with and without ripple, showing increase of deeply trapped particle loss due to combined effect of modes and ripple.

In Fig 9a are shown the resonance locations of all modes for particles with $\mu B = 800keV$, with those for co-moving passing and trapped particles shown in black and those for counter-moving particles in red. The loss boundary for the co-moving particles is the right half of the parabola labeled R, and that for counter-moving particles the left half of the smaller parabola labeled L. We note that resonances for the co-moving passing particles are all deep in the plasma core, far away from the loss boundary, whereas the resonances for the counter-moving passing particles are at the loss boundary, with strong losses predicted around 1200 keV,

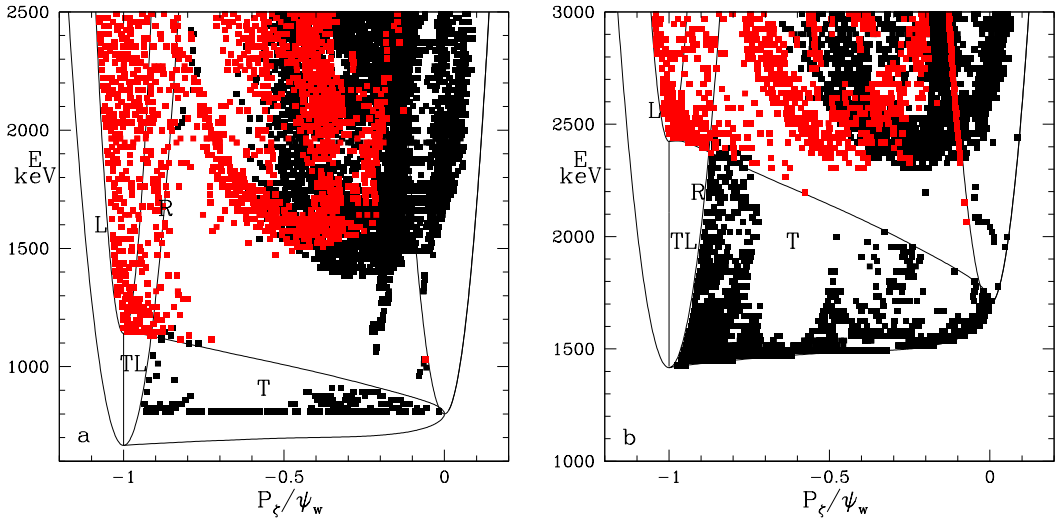

FIG. 9: Mode resonances for all modes, for both the co-moving and counter-moving passing particles and trapped particles, in (a) for $\mu B = 800keV$ and in (b) for $\mu B = 1700keV$. The co-moving and trapped particle resonances are shown in black and the counter-moving resonances in red. The resonance of the co-moving particles are far away from the loss boundary (R), but some of the resonances for the counter-moving particles are located at the loss boundary (L).

many into the domain of trapped loss particles (TL), and also above 2000 keV. Essentially all of these losses are due to the global $n = 1$ mode. The higher n value modes produce the resonances located deep within the plasma, but do not contribute to loss. There are also resonances for trapped particles (T) near the loss boundary at the lower limit of $E = 800keV$. Since this simulation was for $\mu B = 800keV$ energies below this are not possible, but losses at lower energies are most probably present for lower values of μB, contributing to the observed losses peaked at 500 keV.

In Fig 9*b* are shown the resonance locations of all modes for particles with $\mu B = 1700keV$, with those for co-moving passing and trapped particles shown in black and those for counter-moving particles in red. The loss boundary for the co-moving particles is the parabola labeled R, and that for counter-moving particles the smaller parabola labeled L. Again we note that resonances for the co-moving passing particles are all deep in the interior of the plasma, far away from the loss boundary, whereas the resonances for the counter-moving passing particles are at the loss boundary, with strong losses predicted around 2500 keV, many into the domain of trapped loss particles (TL). Large differences in the existence of

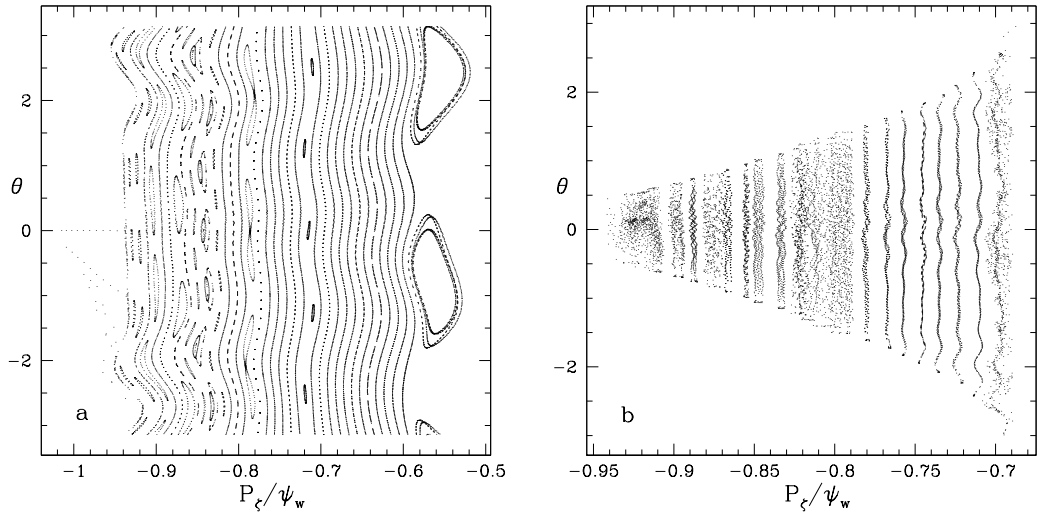

FIG. 10: Kinetic Poincaré plots showing resonances producing losses in the counter-moving passing domain(a) due to the 137 kHz mode with $n = 1$, and in the trapped domain (b) due to the 73 kHz mode with $n = 2$.

resonances are expected, see Eq. 9, but a simple reason for the co-moving particles to resonate only deep within the core is not obvious. Only the low n modes, with $n = 1, 2$ contribute to the loss of counter-moving passing particles, the higher n value modes only produce resonances with these particles deep within the plasma core.

There are also resonances in the trapped particle domain (T), along the boundary with trapped loss, leading to significant loss of trapped particles. All modes contribute to this loss of trapped particles. We conclude that the only induced losses by the modes are on the counter-passing population and the trapped particle population, with co-moving passing particles not participating in mode resonance leading to loss. Furthermore the low n modes are the most dangerous, and in particular the global $n = 1$ mode produces most of the loss of the counter passing particles.

In Fig. 10 are shown examples of the resonances producing loss in the counter passing domain, due to the 137 kHz $n = 1$ mode (a), and in the trapped domain, due to the 73 kHz $n = 2$ mode (b). Kinetic Poincaré plots are capable of examining only a single mode at a time, along a line $E - P_\zeta \omega/n = c$. The plot for the counter passing trajectories was initiated at $E = 1200$ keV. In the counter passing domain many bands of islands are observed near the plasma edge, corresponding to the resonant domain seen in Fig. 9, producing direct loss

of particles due solely to the $n = 1$ mode. The plasma boundary is at P_ζ/ψ_w = -1.1 and all points to the left of P_ζ/ψ_w = -.93 were directly lost indicating that this region is fully stochastic. Farther away from the plasma edge good KAM surfaces exist, and thus there is no loss from deeper within the plasma. The trapped particle plot, initiated at 1600 keV, shows a more complex structure, with a large number of small stochastic resonance bands extending some distance from the plasma boundary, again capable of producing loss. In addition similar structure is seen for several modes with $n > 1$. The combined effect of these modes produces the large band of resonances seen in Fig. 9, leading to losses from some distance within the plasma.

VII. CONCLUSION

An examination of proposed ITER hybrid equilibria and a calculation of spectra of saturated TAE modes produced by alpha particle and beam profiles shows that only very small nonintersecting resonance islands are produced, much too small to make noticable changes in the alpha or beam profiles, and in fact much smaller than the cyclotron radius of the alpha particles. The larger size of ITER and the large field strength, and the consequent small drift excursions of orbits produces resonant islands much smaller and less numerous than what was observed in DIII-D[2, 3]. We conclude that for these equilibria the threat of profile modification by TAE instabilities is nonexistent.

But in the case of an advanced reversed shear equilibrium the situation is somewhat different. Here losses of over one percent can be produced by the combined effect of the predicted TAE mode spectrum and magnetic field ripple. The ripple only adds a small amount to the induced losses, but it is worth remembering that these results rely on the TRANSP deduced alpha particle profile and the predicted magnetic shim reduced ripple magnitude. If this profile is significantly broadened by sawtooth activity or if the ripple is in fact larger the results would be very different. Also if in fact the estimates for TAE mode saturation are too small the losses and profile modification could be much stronger. An analysis of the existing mode-particle resonances determined which modes are responsible for the profile modification. We find that losses are entirely due to resonance with the counter-moving and trapped particle populations, with co-moving passing particles participating in resonances only deep within the plasma, providing some profile modification but not leading

to loss. The dominant loss of counter passing particles is produced by the global low n modes, predominantly the large $n = 1$ mode, with all modes participating in the induced loss of trapped particles.

We should note that the method used is based on the linear theory and inheritably perturbative, that is the TAE/RSAE spectrum and mode structure are given by the MHD theory and their modifications by the particle distributions are not taken into account. This is justified by the relatively low values of their amplitudes used as predicted by the nonlinear theory and by the absence of the wave-particle resonance overlapping. Because of this low amplitude approximation the used approach excludes such known phenomena as EPMs (Energetic Particle Modes). For them to be included one would need to rely on strong modifications of the mode structures such as in the case of n=m=1 fishbones or nonperturbative AEs [19], which have characteristic large mode amplitudes and beyond the perturbative approach. We also do not consider such nonperturbative effects as the possible phase alignment between the modes. This again seems unlikely given the low mode amplitude and the isolation of the separate mode particle resonances.

The offered approach to the fast ion relaxation work should benefit from the studies of the nonlinear evolutions of the Alfvenic modes to confirm or to question the applicability of the used perturbative theory. The modification of the TAE/RSAE mode structures and spectrum can be addressed if important. The most natural way for further studies would be to develop a quasilinear theory such as described in Ref [20].

Acknowledgement

This work was partially supported by the U.S. Department of Energy Grant DE-AC02-09CH11466.

---

[1] W. W. Heidbrink, *Phys. Plasmas* **15**, 055501 (2008), and references therein.

[2] R. B. White, N. N. Gorelenkov, W. W. Heidbrink, M. A. Van Zeeland, *Phys. of Plasmas* **17** 056107 (2010)

[3] R. B. White, N. N. Gorelenkov, W. W. Heidbrink, M. A. Van Zeeland, *Plasmas Physics Controlled Fusion* **52** 045012 (2010)

[4] M. A. Van Zeeland et al, *Phys. of Plasmas* **xx** xxx (2011)

[5] E. P. Fredrickson et al, *Phys. of Plasmas* **16** 122505 (2009)

[6] R.J. Goldston, R. B. White, A.H. Boozer *Phys. Rev. Lett.* **47** 647 (1981)

[7] Y. Gribov,

`ftp://pfctrl@ftp.jp.iter.org/array1/PFcontrol/EQDSKfiles/Code PET/Scenario 4beta scanPET/`

[8] M. A. Van Zeeland et al *Nuclear Fusion* **52** 094023 (2012)

[9] H. L. Berk, B. N. Breizman and M. S. Pekker, *Plasma Phys. Reports*, **23** 778 (1997)

[10] N. N. Gorelenkov, Y. Chen, R. B. White and H. L. Berk, *Phys. Plasmas*, **6** 629 (1999)

[11] R. V. Budny, M. G. Bell A. C. Janos *et al*, *Nucl Fusion* **35**, 1497 (1995).

[12] Alexei Pankin, Douglas McCune, Robert Andre, Glenn Bateman, and Arnold Kritz, *Comp. Phys. Comm.* **159**, 157 (2004).

[13] N. N. Gorelenkov, H. L. Berk, R. V. Budny et.all., Preprint: PPPL-4287, 2008.

[14] A. N. Kolmogorov, *Proc. Int. Congr. Mathematicians, Amsterdam, Vol 1* 315 (1957), V. I. Arnold, *Russ. Math. Surv.* 18(5):9, 1963, J. Moser, *Math. Phys. Kl. II 1,1 Kl(1):1*, 1962.

[15] R. B. White, *The Theory of Toroidally Confined Plasmas, revised second edition*, Imperial College Press, p. 73 (2006)

[16] R. B. White, M.S. Chance, *Phys. Fluids* **27**, 2455 (1984).

[17] R. B. White *Commun. Nonlinear Sci. Numer. Simulat.* **CNSNS** 1906 (2011)

[18] R. B. White *Plasma Phys. Control. Fusion* **53** 085018 (2011)

[19] N. N. Gorelenkov, C. Z. Cheng, W. M. Tang, Phys. Plasmas v.5, (1998) 3389

[20] H. L. Berk, B. N. Breizman, J. Fitzpatrick, H. V. Wang, Nucl. Fusion, V. 35 (1995) 1661.

The Princeton Plasma Physics Laboratory is operated
by Princeton University under contract
with the U.S. Department of Energy.

Information Services
Princeton Plasma Physics Laboratory
P.O. Box 451
Princeton, NJ 08543

Phone: 609-243-2245
Fax: 609-243-2751
e-mail: pppl_info@pppl.gov
Internet Address: http://www.pppl.gov